

RESEARCH

Open Access



# LncRNA LYPLAL1-AS1 rejuvenates human adipose-derived mesenchymal stem cell senescence via transcriptional *MIRLET7B* inactivation

Yanlei Yang<sup>1,2</sup>, Suying Liu<sup>1</sup>, Chengmei He<sup>1</sup>, Taibiao Lv<sup>1</sup>, Liuting Zeng<sup>1</sup>, Fengchun Zhang<sup>1\*</sup>, Hua Chen<sup>1\*</sup> and Robert Chunhua Zhao<sup>2,3\*</sup>

## Abstract

**Background:** Mesenchymal stem cell (MSC) senescence is a phenotype of aging. Long noncoding RNAs (lncRNAs) are emerging as potential key regulators of senescence. However, the role of lncRNAs in MSC senescence remains largely unknown.

**Results:** We performed transcriptome analysis in senescent human adipose-derived MSCs (hADSCs) and identified that the lncRNA LYPLAL1 antisense RNA1 (LYPLAL1-AS1) was significantly downregulated in senescent hADSCs. LYPLAL1-AS1 expression in peripheral blood was lower in middle-aged healthy donors than in young adult donors, and correlated negatively with age. Knockdown of LYPLAL1-AS1 accelerated hADSC senescence, while LYPLAL1-AS1 overexpression attenuated it. Chromatin isolation by RNA purification (ChIRP) sequencing indicated that LYPLAL1-AS1 bound to the *MIRLET7B* promoter region and suppressed its transcription activity, as demonstrated by dual-luciferase assay. miR-let-7b, the transcript of *MIRLET7B*, was upregulated during hADSC senescence and was regulated by LYPLAL1-AS1. Furthermore, miR-let-7b mimics promoted hADSC senescence, while the inhibitors repressed it. Finally, LYPLAL1-AS1 overexpression reversed miR-let-7b-induced hADSC senescence.

**Conclusions:** Our data demonstrate that LYPLAL1-AS1 rejuvenates hADSCs through the transcriptional inhibition of *MIRLET7B*. Our work provides new insights into the mechanism of MSC senescence and indicates lncRNA LYPLAL1-AS1 and miR-let-7b as potential therapeutic targets in aging.

**Keywords:** hADSCs, Senescence, LYPLAL1-AS1, *MIRLET7B*, miR-let-7b

## Introduction

Aging and aging-related chronic diseases such as cardiovascular and cerebrovascular diseases, central nervous diseases, and degenerative osteoarthritis are increasingly burdensome health issues. Stem cell exhaustion, impaired proliferation, and regenerative capacity are important causes of physiological and pathological aging [1, 2]. Mesenchymal stem cells (MSCs) originate in the mesoderm and are isolated from diverse tissues including adipose [3], bone marrow [4], the umbilical cord [5], and

\*Correspondence: zhangfccra@aliyun.com; chenhua@pumch.cn; zhaochunhua@ibms.pumc.edu.cn

<sup>1</sup> Department of Rheumatology and Clinical Immunology, Peking Union Medical College Hospital, Clinical Immunology Center, Chinese Academy of Medical Sciences and Peking Union Medical College, The Ministry of Education Key Laboratory, Beijing, China

<sup>2</sup> Institute of Basic Medical Sciences Chinese Academy of Medical Sciences, School of Basic Medicine Peking Union Medical College, Peking Union Medical College Hospital, Center of Excellence in Tissue Engineering Chinese Academy of Medical Sciences, Beijing Key Laboratory (No. BZO381), Beijing, China  
Full list of author information is available at the end of the article



peripheral blood [6]. MSC populations and pools also decline with age, contributing to human aging and age-related diseases [7].

Given their self-renewal properties, multilineage differentiation potential, and extensive immunomodulatory effects, MSCs are promising tools for cell-based therapies for various diseases, including hematological diseases, autoimmune diseases, peripheral nerve injuries, cardiovascular diseases, and pulmonary infection [8–11], with numerous clinical trials currently underway [12], which demands extensive expansion of MSCs in vitro. However, like other cell types, MSCs undergo senescence in culture. Therefore, elucidating the molecular mechanisms of MSC senescence is essential for stem cell-based therapy in translational medicine.

Acquired senescence such as replicative senescence following extensive passaging including cell cycle arrest, impaired function, or loss of the regenerative phenotype limits the use of MSCs in aging-related disease [13–16]. Cellular senescence is a complex and potentially irreversible process driven by oxidative stress, DNA damage, telomere shortening, and oncogene activation [16]. Although MSCs have significant proliferative potential, they, as with other cells, present replicative senescence after multiple divisions, which is promoted by oxidative stressors such as hydrogen peroxide ( $H_2O_2$ ) [17]. Senescent MSCs exhibit enlarged and granular morphology, deficient cell proliferation and differentiation capacity, produce the senescence-associated secretory phenotype (SASP), and have increased senescence-associated beta-galactosidase (SA- $\beta$ -Gal) activity [16, 18]. The complex underlying mechanisms and regulatory networks of senescence remain to be fully elucidated. The P53–P21 and PRB–P16 pathways are two complementary senescence regulatory pathways that trigger and maintain cellular senescence [19].

Long noncoding RNAs (lncRNAs) are transcripts longer than 200 bp that lack protein-coding capacity. They are emerging as important and divergent regulators in biological processes through their interaction with chromatin modifiers, DNA, RNA, and RNA-binding proteins (RBPs) [20, 21]. Accumulating evidence shows that lncRNAs are altered during aging and senescence stimulation [22, 23]. A recent study using transcriptome profiling and loss-of-function screening showed that lncRNA-OIS1 is essential for oncogene-induced human fibroblast senescence by regulating CDKN1A and DPP4 [24]. Dong et al. revealed that lncRNA CYP7A1-1 is upregulated with age in human bone marrow-derived MSCs and that downregulating CYP7A1-1 rejuvenated aged bone marrow-derived MSCs through *SYNE1* [25]. However, the role of lncRNAs in MSC senescence remains largely unknown.

In the present study, we profiled the transcriptome in senescent human adipose-derived MSCs (hADSCs). We found that lncRNA LYPLAL1-AS1 was significantly downregulated in senescent hADSCs and was inversely associated with the age of healthy donors. We also demonstrate that LYPLAL1-AS1 was a negative regulator of hADSC senescence, which was potentially mediated by downregulating miR-let-7b levels by suppressing *MIRLET7B* promoter activity. Our findings provide new insight into the underlying mechanism of hADSC senescence and indicate potential therapeutic targets in anti-aging.

## Materials and methods

### Cell culture and differentiation

Human adipose-derived MSCs (hADSCs) were isolated from adipose tissues of healthy donors undergoing liposuction as described previously [26–28]. All experiments and procedures were approved by the Ethics Committee of Peking Union Medical College Hospital. hADSCs were maintained at a density of  $1.7 \times 10^5$  cells/ml in a 75 cm<sup>2</sup> flask at 37 °C, 5% CO<sub>2</sub> and were passaged with trypsin/EDTA on 90% confluence as we previously described in detail [29].

For adipogenic differentiation, hADSCs were incubated in adipogenic differentiation medium containing high glucose-DMEM (Gibco) supplemented with 10% FBS (Gibco), 1  $\mu$ M dexamethasone (Sigma-Aldrich), 0.5 mM isobutylmethylxanthine (Sigma-Aldrich), and 1 mM ascorbic acid (Sigma-Aldrich) [30]. Adipogenic differentiation efficiency was determined by oil red O (Sigma-Aldrich) staining [31].

For osteogenic differentiation, hADSCs were incubated in H-DMEM supplemented with 10% FBS, 10 mM  $\beta$ -glycerophosphate (Sigma-Aldrich), 0.5 mM L-ascorbic acid (Sigma-Aldrich), and 0.01 mM dexamethasone [31]. ALP staining using ALP staining kit (Institute of Hematology and Blood Diseases Hospital, Chinese Academy of Medical Sciences, Tianjin, China) and Alizarin red staining [31] were used to measure osteogenic differentiation.

### Flow cytometry

hADSCs at passage 3 and passage 10 were harvested with 0.05% trypsin-EDTA and washed twice using PBS (Servicelbio) and then were incubated with phycoerythrin (PE)-conjugated antibodies against CD29, CD73, CD44, CD90, CD105, CD206, CD34, CD45, CD106, and HLA-DR, FITC-conjugated CD206 or isotype control antibodies (BD Biosciences) for 20 min at 4 °C in dark. Cells were washed twice and were analyzed on Accuri C6 flow cytometer (BD Biosciences) with CFlow Plus software (BD Biosciences)[29].

### Induction of hADSCs senescence

For replicative senescence, hADSCs were continuously cultured in normal medium in 75 cm<sup>2</sup> flask and were passaged at 1:2 ratio normally following the hADSCs culture steps [29]. For H<sub>2</sub>O<sub>2</sub>-induced senescence, hADSCs at 70% confluence were treated with hydrogen peroxide (H<sub>2</sub>O<sub>2</sub>) (100 nM, 300 nM, and 500 nM) for 2 h [32], then cells were washed with PBS and were incubated in fresh media for 24–48 h. Cell senescence was evaluated by  $\beta$ -galactosidase assay using senescence  $\beta$ -galactosidase staining kit (YEASEN, Shanghai, China) according to manufacturer's instructions. Briefly, cells were fixed for 15 min at room temperature in 4% paraformaldehyde, washed twice with PBS, then were incubated with SA- $\beta$ -gal staining working solution overnight at 37 °C without CO<sub>2</sub> in dark. The positive cells were stained blue, and images were acquired using an inverted microscope (Olympus, Japan).

### Clinical samples

Peripheral blood samples of healthy donors (n = 42) were provided by Peking Union Medical College Hospital. The study protocol was approved by the Ethics Committee of Peking Union Medical College Hospital and written informed consent was provided by all donors. The demographic data of donors was listed in Additional file 6: Table S1.

### Cell transfection

siRNA-NC, siRNA-LYPLAL1-AS1, mimics-NC, mimics-miR-let-7b, inhibitors-NC, inhibitors-miR-let-7b, at concentrations of 50 nM were transfected into hADSCs using lipofectamine 2000 (Invitrogen) according to manufacturer's protocol and as we previously described [29]. After 24–48 h of transfection, the hADSCs were collected for further analysis.

For overexpression, full-length LYPLAL1-AS1 was inserted into the LV5-EF1-a-EGFP-Puro lentivirus expression vector and packaged by GenePharma (Shanghai, China), and a lentiviral vector that expressed scrambled RNA was used as the negative control. hADSCs were infected with viral precipitates at a multiplicity of infection of 10, and stable cell lines were established by puromycin treatment as described previously [29].

### RNA extraction and quantitative real-time polymerase chain reaction (qRT-PCR)

Whole blood RNA was extracted by the MolPure Blood RNA Kit (YEASEN, Shanghai) according to manufacturer's instructions. Total RNA of cultured cells was extracted using TRIzol (Invitrogen) according to manufacturer's instructions. cDNA was synthesized using

M-MLV Reverse Transcriptase kit (Takara, Japan). qPCR was performed using SYBR-Green Master mix (YEASEN, Shanghai, China) on an QuantStudio Design & Analysis system (ABI, USA). Relative RNA levels were normalized to GAPDH expression using 2<sup>- $\Delta\Delta$ Ct</sup> method.

For miRNA detection, primers of miR-let-7b used for reverse transcription and qRT-PCR were designed by Sango Biotech (Shanghai, China), U6 was served as internal control. The primer sequences were listed in Additional file 6: Table S2.

### Transcriptome RNA sequencing

hADSCs from three donors were maintained in 6-well plates and were harvested at passage 3 and passage 10. RNA was extracted and library preparations and sequencing was processed on a HiSeq 4000 platform by Novogene (Beijing, China). Differential expression analysis was performed using the DESeq2 R package (1.20.0) with a false discover rate (FDR) cutoff of 0.05. The resulting P-values were adjusted using the Benjamini and Hochberg's approach for controlling the false discovery rate.  $|\log_2\text{FoldChange}| \geq 2$  and adjusted P-value < 0.05 were chosen as the cutoff criteria for differentially expressed genes. The RNA-Sequencing data is available at NCBI under SRA accession number PRJNA803433.

### Subcellular fractionation

Nuclear and cytosolic fractions was extracted using NE-PER Nuclear and Cytoplasmic Extraction Reagents (Thermo Fisher Scientific, USA) according to manufacturer's instructions [33]. RNA was extracted and qRT-PCR was performed to assess the relative expression in nuclear and cytoplasmic fractions.

### Fluorescent in situ hybridization (FISH) assay

FISH was performed using an RNA FISH kit (RiboBio, China) as described previously [29]. Briefly, hADSCs cultured on coverslips were rinsed in PBS and fixed with 4% formaldehyde for 10 min. Cells were permeabilized in PBS containing 0.5% Triton X-100 at 4 °C for 5 min, washed three times, and prehybridized at 37 °C for 30 min. Then, anti-LYPLAL1-AS1, anti-U6, or anti-18S oligodeoxynucleotide probes (RiboBio, China) diluted in hybridization solution were incubated with cells in dark at 37 °C overnight. Cells were stained with DAPI and were imaged using a fluorescence microscope (Carl Zeiss, Germany).

### Chromatin isolation by RNA purification

#### (ChIRP)-sequencing

hADSCs were subjected to ChIRP assay as described [29, 34]. Briefly, Antisense RNA probes were designed (Aksomics, China) to bind every 100 bp of LYPLAL1-AS1

and U1 (positive control) transcripts, with BiotinTEG biotin label conjugated to 3'end. hADSCs ( $2 \times 10^7$ ) were fixed with 1% glutaraldehyde for RNA-chromatin cross-linking, and were snap-frozen in liquid nitrogen and stored at  $-80^\circ\text{C}$ . Samples were added to lysis buffer supplemented with protease inhibitor PMSF at room temperature, and cross-linked DNA-RNA complexes were sonicated until cell lysate was clear to break DNA into 100–500 bp fragments. Cell lysate was hybridized with biotinylated RNA probes. The extraction and subsequent analysis of RNA, DNA, and nucleic acid-binding proteins were performed. Sequencing analysis was performed by Aksomics (Shanghai, China). Sequence reads were generated from Illumina HiSeq 4000, image analysis and base calling were performed using Off-Line Basecaller software (OLB V1.8.0). After passing Solexa CHASTITY quality filter, the clean reads were aligned to Human genome (HG19) using BOWTIE software (V2.1.0); The mapped reads were used for peak detection by MACS V1.4.2 (Model-based Analysis of ChIRP-Seq) software. Statistically significant ChIRP-enriched regions (peaks) were identified by comparison of IP vs Input or comparison to a Poisson background model (Cut-off  $p\text{-value} = 10^{-5}$ ); The GO categories are derived from Gene Ontology ([www.geneontology.org](http://www.geneontology.org)); Pathway analysis are based on the latest KEGG (Kyoto Encyclopedia of Genes and Genomes) database. The ChIRP-sequencing data is available at NCBI under SRA accession number PRJNA788657.

#### Western blot

Protein was extracted using RIPA buffer with PMSF (1:100, Beyotime, China) and was quantified with BCA Protein Assay kit (Beyotime, China). Western blotting was performed in triplicates as previously described [33]. The following antibodies were used: P16 (1:1000, rabbit IgG; Proteintech, 10883-1-AP), P21 (1:1000, rabbit IgG; Proteintech, 10355-1-AP), P53 (1:1000, rabbit IgG; Proteintech, 10442-1-AP), LMNB1 (1:1000, mouse IgG; Proteintech, 66095-1-Ig). Horseradish peroxidase (HRP)-conjugated anti-rabbit-IgG, and HRP-conjugated anti-mouse-IgG (NeoBioscience).

#### Dual-luciferase assay

*MIRLET7B* promoter sequence (2000 bp) was inserted into pGL4 basic luciferase reporter vectors (Promega, USA). Cells ( $5 \times 10^5$ ) were transfected with 0.5  $\mu\text{g}$  expression vector (pGL4-LET7B Promoter or pGL4-Basic), 0.5  $\mu\text{g}$  pCDNA3.1 plasmid (LYPLAL1-AS1 or empty vector) or 5  $\mu\text{l}$  LYPLAL1-AS1 siRNA. *MIRLET7B* promoter activity was normalized by co-transfection with 10 ng of Renilla luciferase reporter. After 48 h, luciferase activity was detected using Dual-Luciferase Reporter Assay

System (Promega, USA). Firefly luciferase activity was normalized to Renilla luciferase activity to yield relative luciferase activity. The *MIRLET7B* promoter sequence was listed in Additional file 6: Table S3, all vectors are constructed by GenePharma (Shanghai, China).

#### Statistical analysis

Data were expressed as mean  $\pm$  standard deviation. Student's t-test and One-way analysis of variance were used for comparisons between two groups and multiple groups, respectively. Statistically significant differences were defined as follows: \* $p < 0.05$ , \*\* $p < 0.01$ , \*\*\* $p < 0.001$ , and \*\*\*\* $p < 0.0001$ . All statistical analysis was performed using GraphPad Prism7 software (GraphPad Prism, San Diego, CA).

## Results

### Characterization of hADSC senescence

hADSCs are fibroblast-like plastic-adherent cells with the potential to differentiate into adipocytes and osteocytes. They express CD29, CD73, CD44, CD90, and CD105 but not CD106, CD206, CD34, CD45, and HLA-DR (Additional file 2: Fig. S1A–E). hADSCs senescence was induced in vitro via serial passaging in culture and  $\text{H}_2\text{O}_2$ -mediated oxidative stress [35, 36]. With increasing passage (P) numbers, the hADSCs gradually exhibited senescent morphology characterized by a flat and irregular shape, and increased SA- $\beta$ -Gal staining (Fig. 1A). The hADSC phenotype remained stable from P3 to P10 (Additional file 2: Fig. S1A, S1B), while senescent hADSCs showed decreased differentiation potential from P3 to P10 (Additional file 2: Fig. S1C–S1E). qRT-PCR revealed that the senescence markers P16 and P21 were significantly increased, while the negative marker LMNB1 was significantly downregulated during hADSC serial passaging (Fig. 1B), which were confirmed by western blotting (Fig. 1C). Furthermore, SA- $\beta$ -Gal-positive hADSCs increased as  $\text{H}_2\text{O}_2$  concentrations increased (Fig. 1D). qRT-PCR confirmed that P16 and P21 were increased while LMNB1 was decreased in  $\text{H}_2\text{O}_2$ -treated hADSCs (Fig. 1E), which was confirmed by western blotting (Fig. 1F). These results indicate that serial passaging and  $\text{H}_2\text{O}_2$ -induced oxidative stress injury drove hADSCs to a senescent state.

### Downregulated LYPLAL1-AS1 in senescent hADSCs

To systematically identify the transcriptome changes involved in hADSC senescence, we performed RNA sequencing analysis of P3 and P10 hADSCs derived from three donors. We identified 25,369 gene transcripts, including 75 upregulated genes and 180 downregulated genes in P10 hADSCs compared with P3 hADSCs (fold change  $\geq 2$ , expression value  $\geq 3$ ,  $p < 0.05$ ) (Fig. 2A).



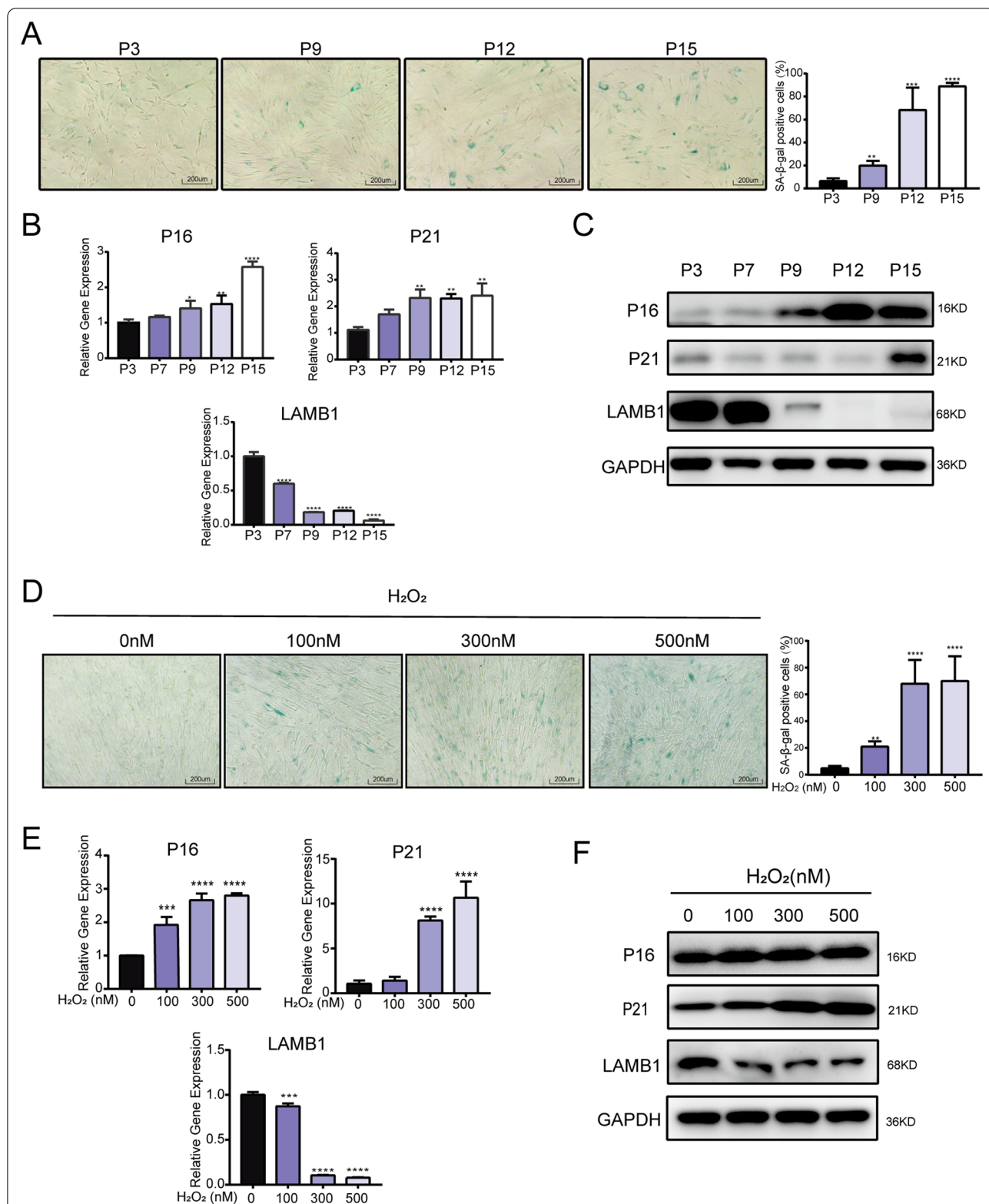


**Fig. 1** Characterization of hADSC senescence. **A** SA-β-Gal staining of hADSCs during replicative senescence at different passage(P): P3, P9, P12, and P15. **B** qRT-PCR of senescence markers *P16*, *P21*, and *LMNB1* in hADSCs during replicative senescence. **C** Western blot of *P16*, *P21*, and *LMNB1* in hADSCs during replicative senescence. **D** SA-β-Gal staining of H<sub>2</sub>O<sub>2</sub>-treated hADSCs. **E** qRT-PCR of *P16*, *P21*, and *LMNB1* in H<sub>2</sub>O<sub>2</sub>-treated hADSCs. **F** Western blot of *P16*, *P21*, and *LMNB1* in H<sub>2</sub>O<sub>2</sub>-treated hADSCs. qPCR data were normalized to *GAPDH*, n = 3. Data are shown as mean ± SD from three independent experiments. \*p < 0.05, \*\*p < 0.01, \*\*\*p < 0.001, \*\*\*\*p < 0.0001; scale bars: 200 μm

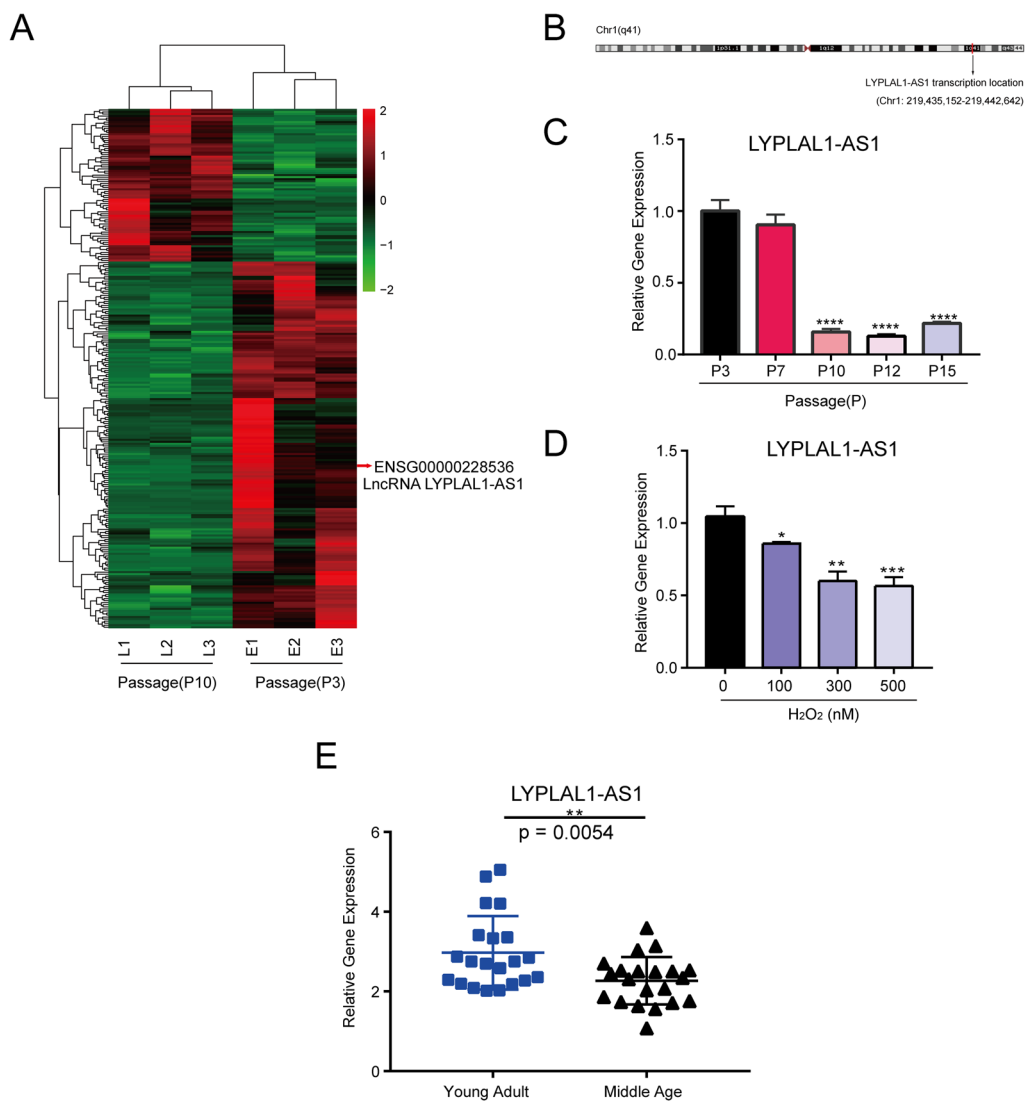


**Fig. 2** Downregulated LYPLAL1-AS1 in senescent hADSCs. **A** Heatmap of differentially expressed genes between P10 and P3 hADSCs from three donors. Red arrow indicates LYPLAL1-AS1. **B** Genomic location of LYPLAL1-AS1. **C** qRT-PCR of *LYPLAL1-AS1* in hADSCs during replicative senescence at different passages. **D** qRT-PCR of *LYPLAL1-AS1* in hADSCs during replicative senescence at different passages. qRT-PCR of *LYPLAL1-AS1* in H<sub>2</sub>O<sub>2</sub>-treated hADSCs. **E** qRT-PCR of *LYPLAL1-AS1* in young adult (median age: 27 years, n = 21) and middle-aged healthy donors (median age: 53 years, n = 21). qPCR data were normalized to *GAPDH*, n = 3. Data are shown as mean ± SD from three independent experiments; \**p* < 0.05, \*\**p* < 0.01, \*\*\**p* < 0.001, \*\*\*\**p* < 0.0001

Among the differentially expressed genes, we noted that a lncRNA, LYPLAL1-AS1, which is transcribed in the opposite direction relative to *LYPLAL1* on chromosome 1, was notably downregulated in senescent hADSCs (Fig. 2A, B). qRT-PCR confirmed that LYPLAL1-AS1 was downregulated in hADSCs during serial passaging (Fig. 2C) and under H<sub>2</sub>O<sub>2</sub> exposure (Fig. 2D). To validate the clinical relevance between LYPLAL1-AS1 and aging, we analyzed its expression in the peripheral blood of young adult (age: 24–28 years, median age: 27 years,

n = 21) and middle-aged adult (age: 49–57 years, median age: 53 years, n = 21) healthy donors (Additional file 6: Table S1). qRT-PCR showed that LYPLAL1-AS1 expression was significantly higher in the young adults compared with the middle-aged adults (*p* = 0.0054) (Fig. 2E) and was inversely correlated with age (*r* = -0.3704, *p* = 0.0158) (Additional file 3: Fig. S2). Together, LYPLAL1-AS1 was downregulated in senescent hADSCs and older people, suggesting as a potential negative regulator of hADSC senescence.

### LYPLAL1-AS1 knockdown accelerates hADSC senescence

To evaluate the role of LYPLAL1-AS1 in hADSC senescence, we first silenced LYPLAL1-AS1 in P10 hADSCs using specific small interfering RNAs (siRNAs) (Fig. 3A). SA- $\beta$ -Gal-positive cells were significantly increased in the LYPLAL1-AS1-silenced hADSCs than in control hADSCs (Fig. 3B). qRT-PCR and western blotting indicated that P16 and P21 were upregulated, while LMNB1 was downregulated in LYPLAL1-AS1-silenced hADSCs (Fig. 3C, D). Furthermore, we silenced LYPLAL1-AS1 in H<sub>2</sub>O<sub>2</sub>-treated hADSCs. Consistent with the earlier results, qRT-PCR and western blotting revealed that LYPLAL1-AS1 knockdown enhanced the senescence effect of H<sub>2</sub>O<sub>2</sub> on hADSCs, as indicated by increased P16 and P21 levels and decreased LMNB1 levels in the LYPLAL1-AS1 knockdown group (Fig. 3E, F), and by the decreased SA- $\beta$ -Gal-positive cells (Fig. 3G). These data demonstrate that LYPLAL1-AS1 downregulation accelerates hADSC senescence.

### LYPLAL1-AS1 overexpression attenuates hADSC senescence

To confirm the role of LYPLAL1-AS1 in hADSC senescence, we overexpressed LYPLAL1-AS1 in hADSCs using lentivirus. The lentiviral transfection efficiency was >90% as determined by green fluorescent protein (GFP) expression (Fig. 4A), and LYPLAL1-AS1 was significantly overexpressed (Fig. 4B). LYPLAL1-AS1 overexpression decreased SA- $\beta$ -Gal staining in senescent hADSCs (Fig. 4C) and impaired P16 and P21 expression while improving LMNB1 expression as detected by qRT-PCR (Fig. 4D) and western blotting (Fig. 4E). Western blotting also showed that LYPLAL1-AS1 overexpression inhibited the senescence effect of H<sub>2</sub>O<sub>2</sub> on hADSCs, as P16 and P21 were decreased and LMNB1 was increased (Fig. 4F), and SA- $\beta$ -Gal-positive cells were decreased (Fig. 4G). Collectively, these data indicate that LYPLAL1-AS1 overexpression inhibits hADSC senescence.

### LYPLAL1-AS1-regulated genes identified by ChIRP-seq

LYPLAL1-AS1 was distributed in both the nucleus and cytoplasm (Fig. 5A and Additional file 4: Fig. S3). To explore the downstream genes regulated by LYPLAL1-AS1, we conducted chromatin isolation by RNA purification sequencing (ChIRP-seq) analysis of LYPLAL1-AS1 in hADSCs to capture its direct binding DNA targets, which showed that LYPLAL1-AS1 bound at the intron, exon, promoter, upstream regions, and intergenic sites (Fig. 5B, C). We performed Gene Ontology (GO) and Kyoto Encyclopedia of Genes and Genomes (KEGG) pathway enrichment analyses on

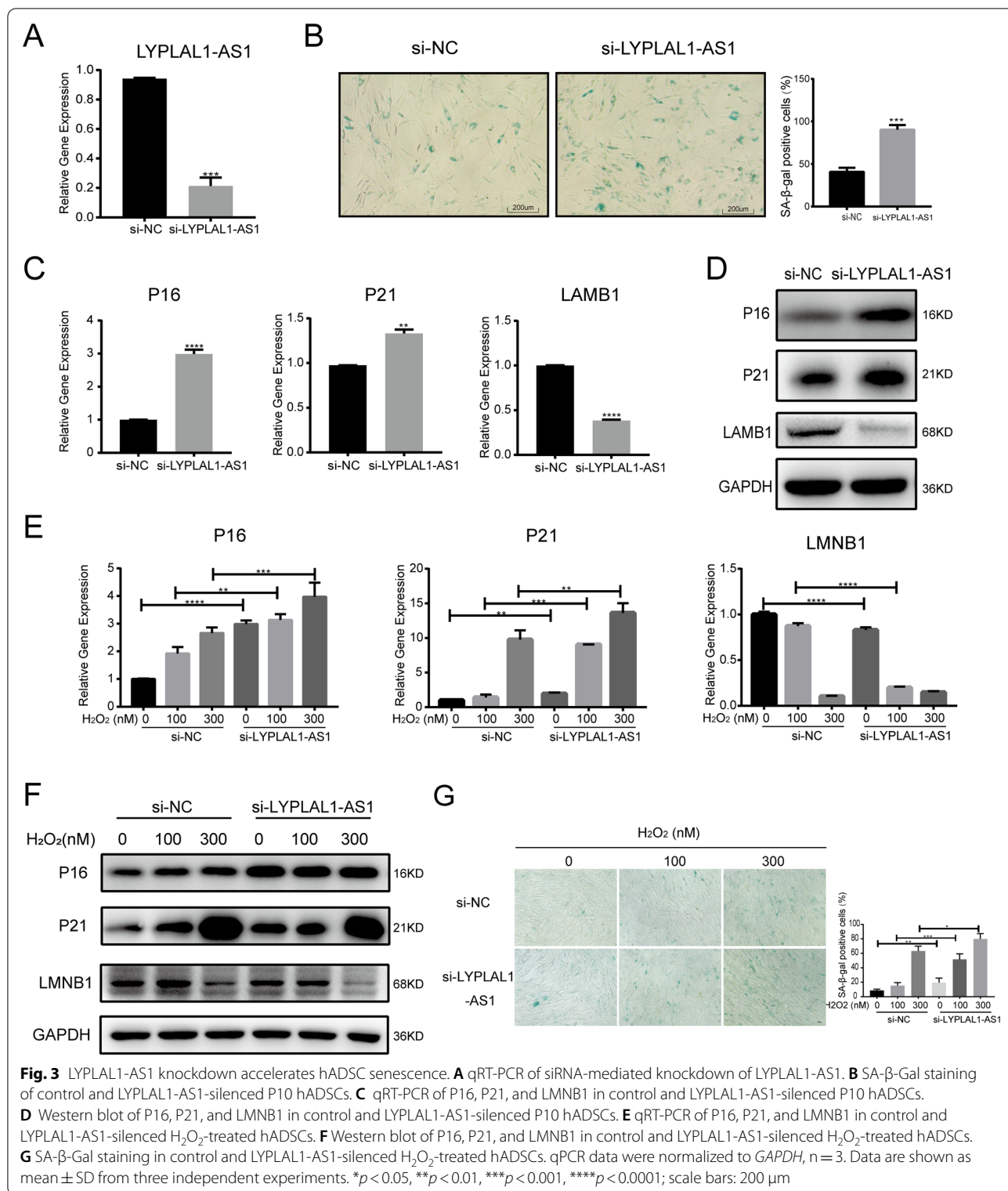
all binding genes. KEGG pathway enrichment analysis suggested that LYPLAL1-AS1 potentially regulated the senescence-related pathways, including the JAK-STAT signaling pathway and the apoptosis pathway (Fig. 5D). GO analysis revealed that the target genes of LYPLAL1-AS1 participated in diverse biological processes, including regulation of oxidative stress-induced genes and regulation of ARF protein signal transduction (Fig. 5E).

### LYPLAL1-AS1 negatively regulates MIRLET7B

ChIRP-seq showed that LYPLAL1-AS1 bound on the *MIRLET7B* promoter in a 1.2-kb window on chr22, which was presented by Integrative Genomics Viewer (IGV) software (Fig. 6A), suggesting that LYPLAL1-AS1 may regulate *MIRLET7B* transcription. *MIRLET7B* is the host gene of miR-let-7b-5p (hereafter referred to as miR-let-7b) that is augmented during oxygen exposure, causing oxidative stress and senescence in the choroid and retinal pigment epithelium through the p53-let-7b-IGF-1R axis [37], but the role of miR-let-7b in cell senescence remains unclear. Accordingly, we aimed to reveal whether *MIRLET7B* and its mature miRNA (miR-let-7b) are involved in LYPLAL1-AS1 repression hADSC senescence. To explore the transcriptional regulatory effect of LYPLAL1-AS1 on *MIRLET7B*, we transfected 293 T cells with *MIRLET7B* promoter-luciferase reporter vectors and LYPLAL1-AS1 expression vectors or empty vectors. The luciferase activity of the *MIRLET7B* promoter decreased as LYPLAL1-AS1 expression increased (Fig. 6B). Silencing LYPLAL1-AS1 induced enhanced *MIRLET7B* promoter-reporter activity (Fig. 6C), confirming that LYPLAL1-AS1 was a negative regulator of *MIRLET7B* promoter. Next, we evaluated whether LYPLAL1-AS1 regulated miR-let-7b expression levels, and profiled miR-let-7b expression during hADSC senescence. qRT-PCR showed that LYPLAL1-AS1 downregulation increased miR-let-7b expression, while LYPLAL1-AS1 upregulation decreased it (Fig. 6D). Accordingly, miR-let-7b expression was markedly increased in hADSCs with serial passaging (Fig. 6E) or H<sub>2</sub>O<sub>2</sub> treatment (Fig. 6F), suggesting that miR-let-7b is a positive regulator of hADSC senescence. Collectively, these data reveal that LYPLAL1-AS1 directly bound to the *MIRLET7B* promoter and potentially downregulates miR-let-7b levels by suppressing *MIRLET7B* promoter activity.

### miR-let-7b promotes hADSC senescence, which is reversed by LYPLAL1-AS1

We explored whether miR-let-7b regulated hADSC senescence by transfecting miR-let-7b mimics, negative



controls (NC), or miR-let-7b inhibitor into hADSCs. The miR-let-7b mimics increased miR-let-7b expression while the inhibitors decreased it (Fig. 7A). The miR-let-7b

mimics promoted SA-β-Gal expression, while the miR-let-7b inhibitors attenuated it (Fig. 7B). The miR-let-7b mimics promoted hADSC senescence as shown by the



upregulated P16 and P21 and downregulated LMNB1, while its inhibitors inhibited hADSC senescence as shown by the downregulated P16 and P21 and upregulated LMNB1 (Fig. 7C, D). The findings suggest that miR-let-7b is a positive regulator of hADSC senescence. To examine whether LYPLAL1-AS1 regulated miR-let-7b-induced hADSC senescence, we overexpressed LYPLAL1-AS1 or control in hADSCs then transfected them with miR-let-7b mimics. LYPLAL1-AS1 overexpression significantly inhibited the upregulated P16 and P21 levels and increased the downregulated LMNB1 level induced by the miR-let-7b mimics (Fig. 7E, F), indicating that LYPLAL1-AS1 reversed miR-let-7b-induced hADSC senescence. Collectively, our data indicate that LYPLAL1-AS1 is a negative regulator of hADSC senescence, potentially through transcriptional modulation of *MIRLET7B* expression.

## Discussion

Elucidating the regulation, intervention, and rejuvenation of MSC senescence is important for MSC-based therapy for anti-aging. Repeated subculture and H<sub>2</sub>O<sub>2</sub> exposure induce MSC senescence, which are suitable models of MSC senescence in vitro [32, 38]. In the present study, we demonstrate that LYPLAL1-AS1 is a negative regulator of hADSC senescence induced by repeated subculture and H<sub>2</sub>O<sub>2</sub> exposure, which was inversely correlated with aging. We also reveal that LYPLAL1-AS1 rejuvenates hADSC senescence through transcriptional inhibition of the *MIRLET7B* promoter.

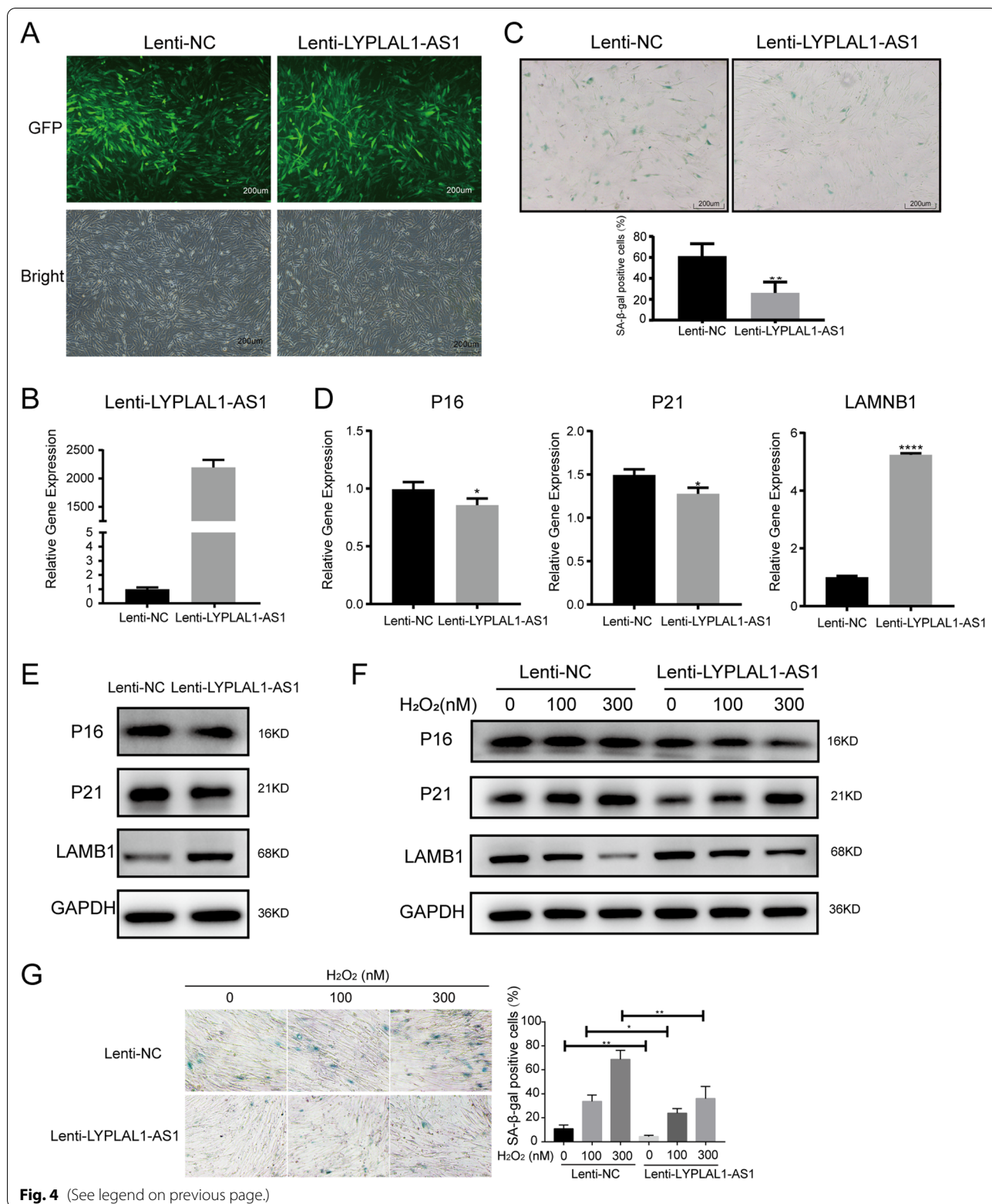
lncRNAs have versatile regulation functions at multiple levels. lncRNA ANCR suppresses epidermal and definitive endoderm differentiation [33] and modulates osteogenic and adipogenic differentiation and tumor progression. lncRNA MEG3 promotes MSC osteogenic differentiation at transcriptional level by acting as a decoy to dissociate SOX2 binding at the *BMP4* promoter to activate BMP4 [39], and acts as a competing endogenous RNA (ceRNA) to regulate osteogenic gene expression at post-transcriptional level [40]. lncRNA-p21 is distributed in both the cytoplasm and nuclear, coordinates with RCK RNA helicase to suppress target mRNA translation in the cytoplasm [41], and methylates and maintains H3K9me3 at the promoters of pluripotent genes to repress their transcription by interacting

with heterogeneous nuclear ribonucleoprotein (hnRNP) K protein [42]. We have reported that LYPLAL1-AS1 is a key promoter of hADSC adipogenic differentiation by directly targeting and modulating DSP protein stability in the cytoplasm [29]. Herein, we demonstrate that LYPLAL1-AS1 participates in regulating hADSCs senescence, which was mediated by the transcriptional inhibition of *MIRLET7B*. Therefore, LYPLAL1-AS1 regulates hADSCs at multiple levels, and other potential functions of LYPLAL1-AS1 on hADSCs remained to be explored. In addition, the function of specific lncRNAs is not restricted to a specific protein and they may influence multiple potential targets in a cell type-dependent way. For instance, lncRNA HOTAIR participates in regulating MSC function, which may cause senescence-associated DNA methylation to impact MSC proliferation and differentiation [43]. In senescent human fibroblasts, HOTAIR is upregulated and prevents premature senescence by causing rapid decay of targets Ataxin-1 and Snurportin-1 [44]. In cancer cell lines, HOTAIR depletion may be correlated with cell cycle arrest by decreasing S phase cells, inhibiting cell proliferation rate, and promoting apoptotic levels [45, 46]. Our study revealed one function of LYPLAL1-AS1 in preventing human adipose-derived-MSC (hADSC) senescence, and besides adipose tissue, LYPLAL1-AS1 also exhibits high expression in ovary, mammary and subcutaneous according to human RNA sequencing (RNA-Seq) expression data from UCSC (<http://genome.ucsc.edu>), therefore, extending our research to other cell types is a promising direction in the future.

MSC senescence is a complex process. Besides the innate molecular dynamic changes in SA- $\beta$ -Gal staining and P16, P21, and LMNB1 expression examined in the present research, their functional abilities might also change, including the differentiation property which is intricately regulated by multiple factors, including transcriptional factors, growth factors, and epigenetic factors such as ncRNAs (miRNAs, lncRNAs) [47–49]. Our previous research indicate that LYPLAL1-AS1 is a key regulator of adipogenic differentiation, promoting the differentiation of normal hADSCs toward adipogenic cells by directly targeting and modulating DSP protein stability [29]. As shown in Additional file 5: Fig. S4A, overexpression of LYPLAL1-AS1 partially reversed the

(See figure on next page.)

**Fig. 4** LYPLAL1-AS1 overexpression attenuates hADSC senescence. **A** Representative images of hADSCs transfected with lentivirus expressing GFP and control (Lenti-NC) or LYPLAL1-AS1 (Lenti-LYPLAL1-AS1). **B** qRT-PCR of overexpression efficiency of LYPLAL1-AS1 in hADSCs transfected with control or LYPLAL1-AS1 overexpression lentivirus. **C** SA- $\beta$ -Gal staining in control and LYPLAL1-AS1 overexpression P10 hADSCs. **D** qRT-PCR of *P16*, *P21*, and *LMNB1* in control and LYPLAL1-AS1 overexpression P10 hADSCs. **E** Western blot of P16, P21, and LMNB1 in control and LYPLAL1-AS1 overexpression P10 hADSCs. **F** Western blot of P16, P21, and LMNB1 in control and LYPLAL1-AS1 overexpression H<sub>2</sub>O<sub>2</sub>-treated hADSCs. **G** SA- $\beta$ -Gal staining in control and LYPLAL1-AS1 overexpression H<sub>2</sub>O<sub>2</sub>-treated hADSCs. qPCR data were normalized to *GAPDH*, n = 3. Data are shown as mean  $\pm$  SD from three independent experiments; \* $p$  < 0.05, \*\* $p$  < 0.01, \*\*\*\* $p$  < 0.0001; scale bars: 200  $\mu$ m



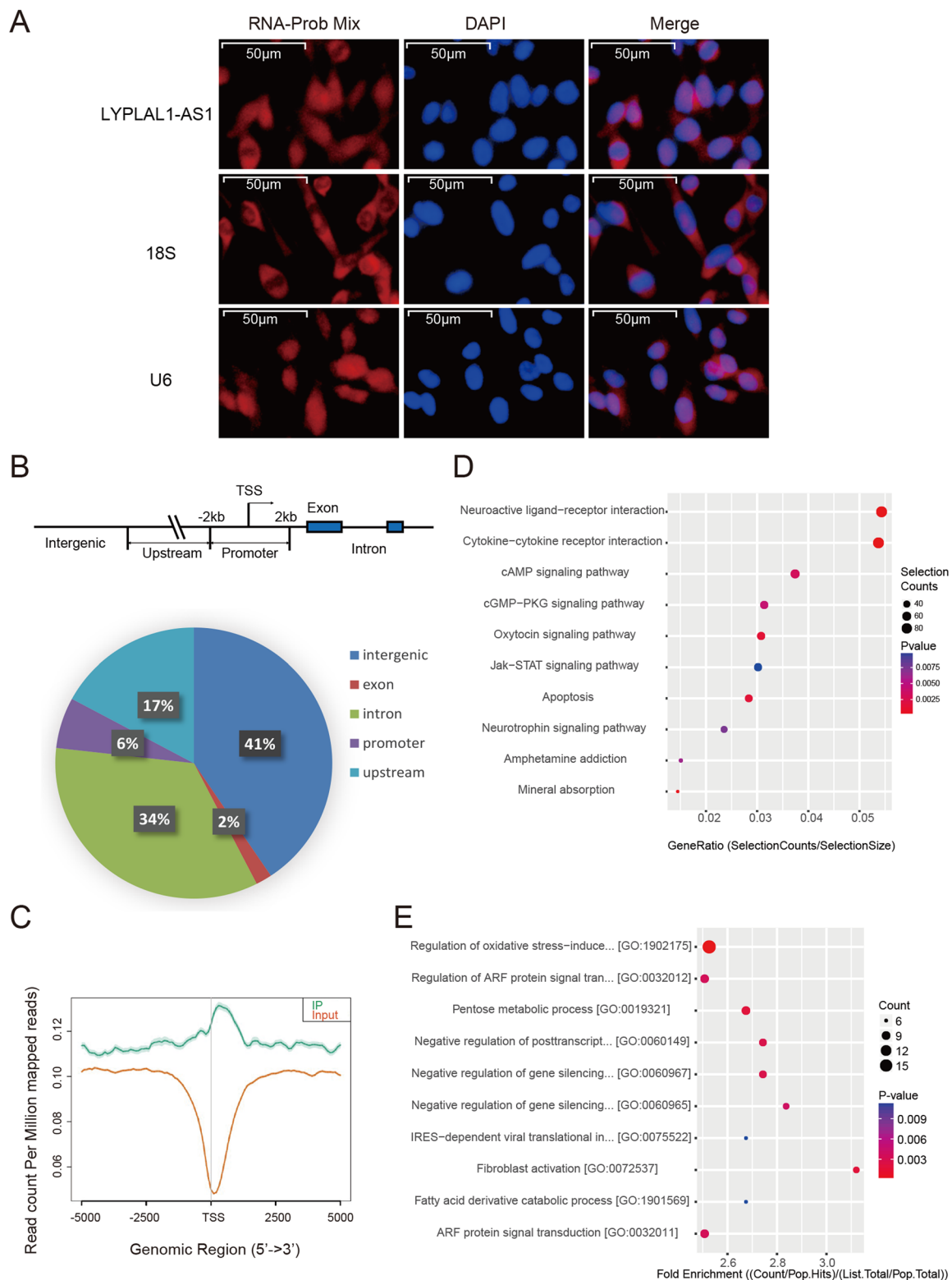
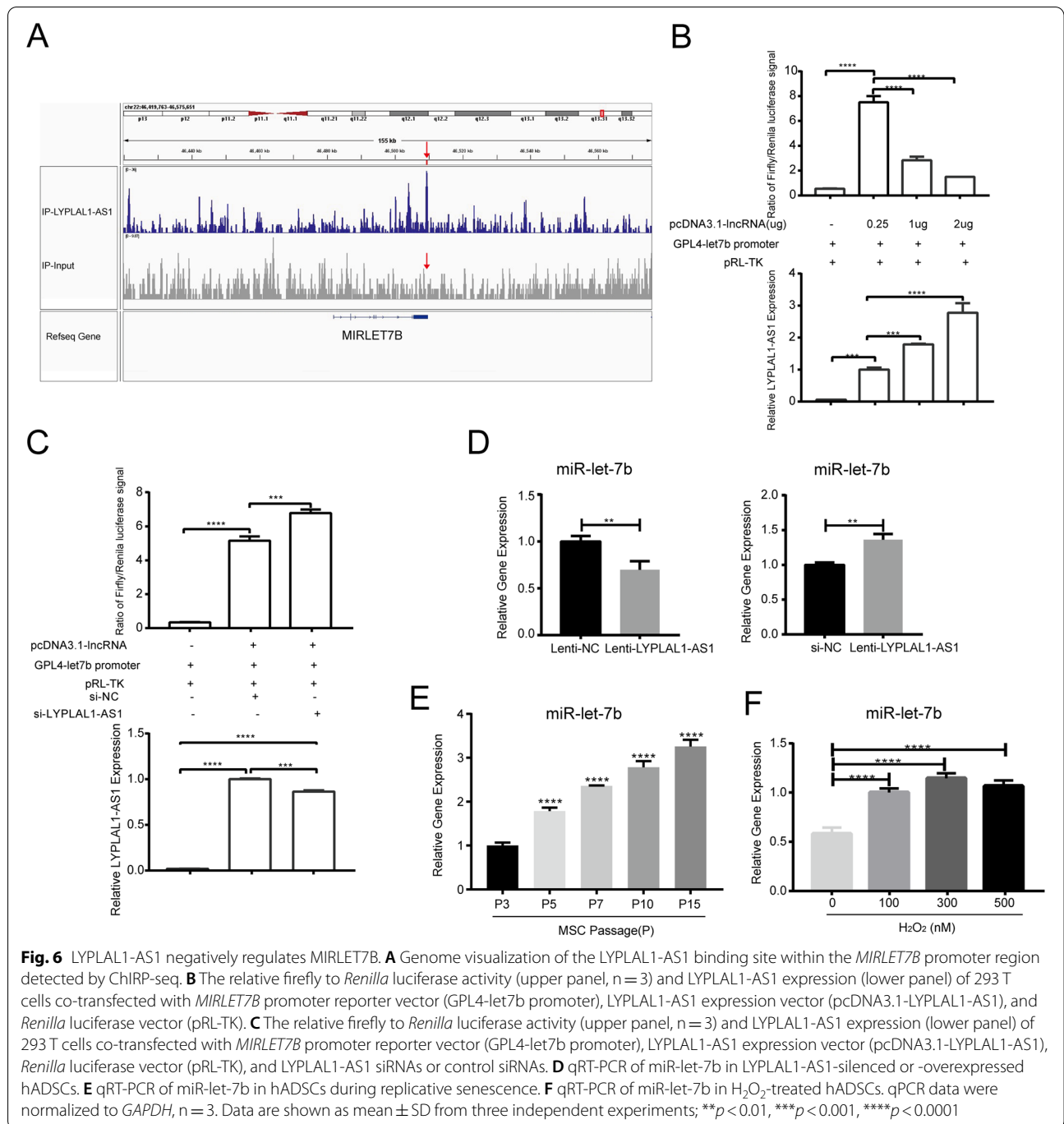


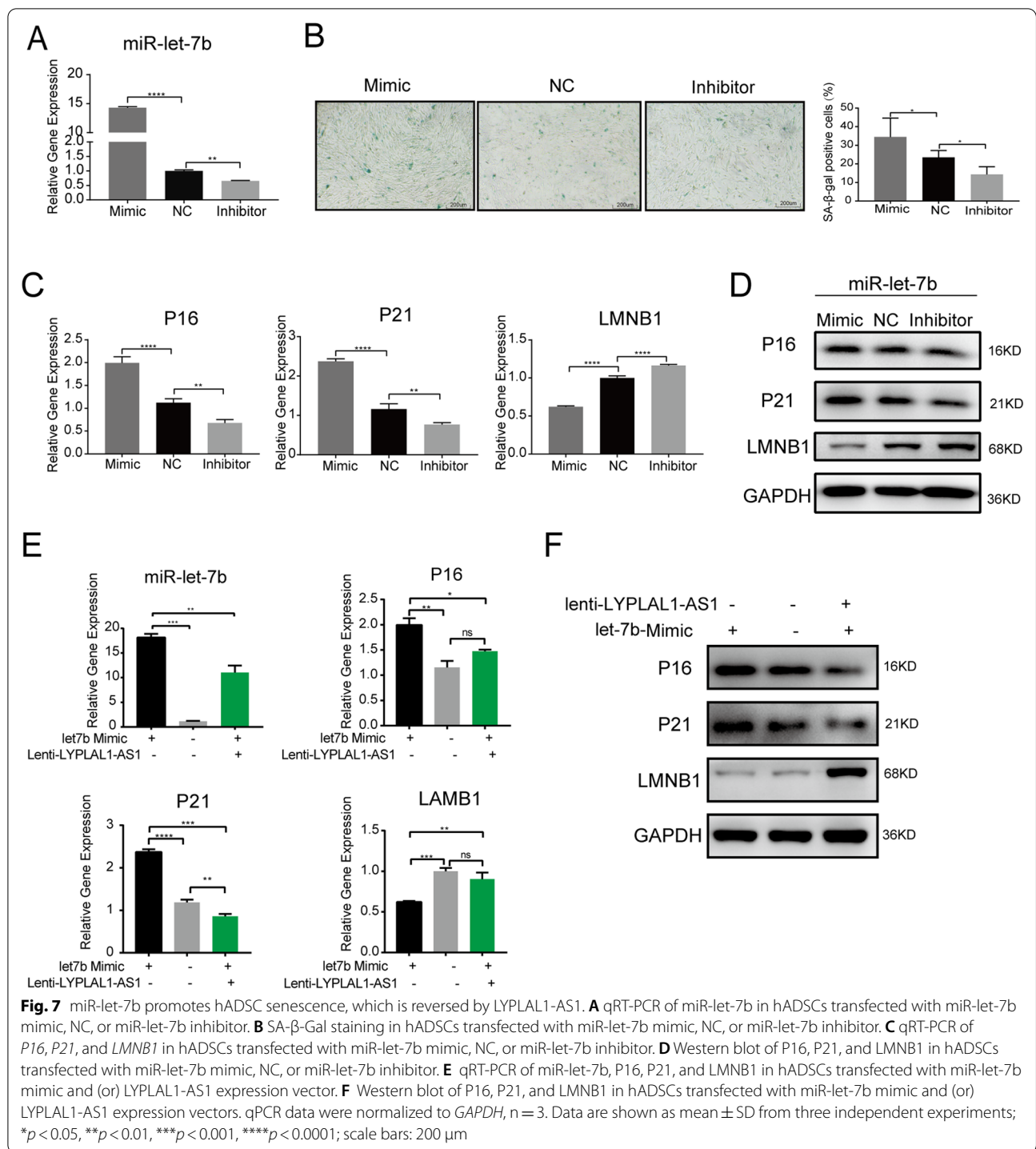
**Fig. 5** LYPLAL1-AS1-regulated genes identified by ChIP-seq. **A** RNA fluorescence in situ hybridization (FISH) assay for LYPLAL1-AS1 in hADSCs. 18S and U6 were the cytoplasmic and nuclear RNA controls, respectively. Scale bars: 50 µm. **B** Diagram of the distribution of LYPLAL1-AS1 binding loci. **C** Distribution of peaks within the transcription start site (TSS) ± 5 kb of the LYPLAL1-AS1 binding-related elements. **D** KEGG pathway analysis of LYPLAL1-AS1-related genes. **E** GO biological process enrichment analysis of LYPLAL1-AS1-related genes



adipogenic differentiation of senescent hADSCs, as indicated by oil red O staining, suggesting that LYPLAL1-AS1 overexpression ameliorates hADSC senescence, resulting in increased cell differentiation potential. The differentiation potential of MSCs changed with senescence [50, 51]. Increasing evidence indicates that senescent MSCs exhibit elevated adipogenesis at the expense of osteogenesis which is consistent with the in vivo

increased bone marrow adiposity in aging, leading to damaged bone formation ability in humans and animals [51–53]. Most studies indicate that osteogenic differentiation potential of MSCs deteriorates with age [38, 54, 55], and the adipogenic differentiation potential of MSCs is disputable. Some studies indicate that the adipogenesis potential of MSCs tends to decline with senescence [56, 57]. In a well-controlled study using rat model, MSCs





undergoing long-term passaging exhibit impaired in vitro differentiation potential including complete loss of osteogenic potential and attenuated adipogenic potential [58]. Other studies indicate the increasing adipogenic potential of senescent MSCs [59–61]. The discrepancy about whether senescent MSCs harbor increased or decreased

adipogenic potential may be due to the different in vitro culture conditions and complex in vivo microenvironment including cell-intrinsic cytokines and hormones. Therefore, cellular senescence might not adequately explain the change in MSC differentiation, and the cell-intrinsic mechanism that regulates the age-related

change in MSC differentiation deserved comprehensive studies in the future. Besides, deficiency in cell proliferation is also a characteristic of senescent MSCs. We also found knockdown and overexpression of LYPLAL1-AS1 had little effect on the proliferation of young (P3) hADSCs (Additional file 5: Fig. S4B, C), while its overexpression significantly reversed the proliferation of senescent hADSCs (Additional file 5: Fig. S4C, D), suggesting that LYPLAL1-AS1 overexpression ameliorates cellular senescence by rejuvenating senescent hADSCs, resulting in increased cell proliferation. Future studies should explore the underlying cellular and molecular defects that may explain the altered cell proliferation in senescent hADSCs.

A common lncRNA–miRNA interaction mechanism is lncRNAs acting as sponges to compete with mRNAs for miRNA binding, also known as the ceRNA mechanism [62–64]. However, TargetScan predicted no binding sequence between LYPLAL1-AS1 and miR-let-7b (data not shown). Combined with the ChIRP-seq analysis showing direct binding between LYPLAL1-AS1 and the *MIRLET7B* promoter, we propose that LYPLAL1-AS1 inhibits *MIRLET7B* promoter activity, thereby indirectly modulating miR-let-7b levels at the transcriptional level. LncRNA regulation of gene transcription has been extensively studied [65, 66]. LncRNAs may act as guides to recruit proteins to DNA through RNA–DNA and RNA–protein interactions [67–69]. Guide lncRNAs have both protein-binding functions and genome-interfacing functions. Here, we reveal that LYPLAL1-AS1 interfaced directly with the *MIRLET7B* promoter and regulate its activity negatively. Further studies are warranted to determine whether other proteins are involved in this process. Therefore, we suggest a new underlying mechanism of LYPLAL1-AS1 inhibition of hADSC senescence: it potentially inhibits the *MIRLET7B* promoter transcriptionally, thereby downregulating miR-let-7b levels.

Similar to protein-coding genes, miRNA host gene promoters contain CpG islands, TATA box sequences, initiation elements, and certain histone modifications that enable their control by transcription factors, enhancers, silencing elements, and chromatin modifications [70, 71]. miRNA processing from the host gene or miRNA precursor transcription may affect mature miRNA levels [72]. Therefore, transcriptional regulation of miRNAs is partially responsible for their specific spatial and temporal expression patterns [73]. For example, p53 promotes miR-34 and miR-107 family expression, which enhances tumor cell cycle arrest and apoptosis [70, 74]. PITX3 stimulates miR-133b transcription and contributes to the maturation and function of midbrain dopaminergic neurons [75]. Herein, we found that LYPLAL1-AS1 downregulated miR-let-7b levels by binding to the

promoter region of its host gene *MIRLET7B* and suppressing transcriptional activity, thereby attenuating hADSC senescence. miR-let-7b is a let-7 family miRNA that is upregulated in the plasma of patients with age-related macular degeneration [76]. A recent study has indicated that miR-let-7b is augmented in choroid and retinal pigment epithelium exposed to oxygen and that increased p53–miR-let-7b activity promotes the inability of the choroid to revascularize in oxygen-induced retinopathy [37]. However, whether miR-let-7b plays a role in hADSC senescence remains unknown. Our data demonstrate that miR-let-7b accelerates hADSC senescence, which is regulated by LYPLAL1-AS1. Therefore, targeting miR-let-7b might be a promising approach for reducing hADSC senescence.

## Conclusions

We demonstrate that LYPLAL1-AS1 rejuvenates hADSCs through the transcriptional inhibition of *MIRLET7B*. Our work provides new insights into the mechanism of stem cell senescence. LYPLAL1-AS1 and miR-let-7b might be potential therapeutic targets in aging-related diseases.

## Supplementary Information

The online version contains supplementary material available at <https://doi.org/10.1186/s13578-022-00782-x>.

**Additional file 1.** Methods and figure legends

**Additional file 2: Figure S1.** Morphological, functional, and phenotype characteristics of hADSCs

**Additional file 3: Figure S2.** Correlation analysis of LYPLAL1-AS1 expression level and age in healthy donors (n=42). data were analyzed using R software version 3.5.3

**Additional file 4: Figure S3.** Subcellular fractionation of LYPLAL1-AS1 in hADSCs followed by qRT-PCR. GAPDH and U6 mRNA served as cytoplasmic and nuclear control, respectively.

**Additional file 5: Figure S4.** LYPLAL1-AS1 overexpression ameliorates cellular senescence, resulting in increased cell differentiation potential and increased cell proliferation. A. Oil red O staining of adipose lipids in at P3 or P10 hADSCs overexpressing LYPLAL1-AS1 or control on day 10 after adipogenic induction. B. Cell proliferation of P3 hADSCs was tested by MTS when LYPLAL1-AS1 was knocked down. C. Cell proliferation of P3 and P10 hADSCs was tested by MTS when LYPLAL1-AS1 was overexpressed. D. Cell cycle analysis of hADSCs transfected with Lenti-NC or Lenti-LYPLAL1-AS1 at P10. (TIF 2176 KB)

**Additional file 6: Table S1.** Demographic data of healthy donors.

**Table S2.** Primer sequences. **Table S3.** *MIRLET7B* promoter sequence (2000bp).

## Acknowledgements

We thank the Institute of Basic Medical Sciences, Chinese Academy of Medical Sciences for providing and maintaining the equipment and technical support needed in our study.

**Author contributions**

RCZ, HC and FCZ conceived the project; YLY designed experiments; YLY, SYL, CMH, ZLC, TBL, LTZ conducted experiments, analyzed and interpreted data; YLY wrote and revised the manuscript. All authors contributed to the discussion of results and the final approval of the version to be published.

**Funding**

This study was supported by China Postdoctoral Science Foundation (2021M690461), National Natural Science Fund (82071842, 81571594, 81771764), National Key R&D Program of China (2016YFA0101003), CAMS Innovation Fund for Medical Sciences (2017-I2M-3-007, 2016-I2M-1-003).

**Availability of data and materials**

The data that support the findings of this study are available from the corresponding author upon reasonable request.

**Declarations****Ethics approval and consent to participate**

All experiments and procedures were approved by the Ethics Committee of Peking Union Medical College Hospital.

**Consent for publication**

Not applicable.

**Competing interests**

The authors declare that they have no competing interests.

**Author details**

<sup>1</sup>Department of Rheumatology and Clinical Immunology, Peking Union Medical College Hospital, Clinical Immunology Center, Chinese Academy of Medical Sciences and Peking Union Medical College, The Ministry of Education Key Laboratory, Beijing, China. <sup>2</sup>Institute of Basic Medical Sciences Chinese Academy of Medical Sciences, School of Basic Medicine Peking Union Medical College, Peking Union Medical College Hospital, Center of Excellence in Tissue Engineering Chinese Academy of Medical Sciences, Beijing Key Laboratory (No. BZO381), Beijing, China. <sup>3</sup>School of Life Sciences, Shanghai University, Shanghai, China.

Received: 20 October 2021 Accepted: 31 March 2022

Published online: 21 April 2022

**References**

- López-Otin C, Blasco MA, Partridge L, Serrano M, Kroemer G. The hallmarks of aging. *Cell*. 2013;153(6):1194–217.
- Oh J, Lee YD, Wagers AJ. Stem cell aging: mechanisms, regulators and therapeutic opportunities. *Nat Med*. 2014;20(8):870–80.
- Zuk PA, Zhu M, Ashjian P, De Ugarte DA, Huang JJ, Mizuno H, Alfonso ZC, Fraser JK, Benhaim O, Hedrick MH. Human adipose tissue is a source of multipotent stem cells. *Mol Biol Cell*. 2002;13(12):4279–95.
- Friedenstein AJ, Gorskaja JF, Kulagina NN. Fibroblast precursors in normal and irradiated mouse hematopoietic organs. *Exp Hematol*. 1976;4(5):267–74.
- Romanov YA, Svintsitskaya VA, Smirnov VN. Searching for alternative sources of postnatal human mesenchymal stem cells: candidate MSC-like cells from umbilical cord. *Stem cells* (Dayton, Ohio). 2003;21(1):105–10.
- Ukai R, Honmou O, Harada K, Houkin K, Hamada H, Kocsis JD. Mesenchymal stem cells derived from peripheral blood protects against ischemia. *J Neurotrauma*. 2007;24(3):508–20.
- Neri S, Borzi RM. Molecular mechanisms contributing to mesenchymal stromal cell aging. *Biomolecules*. 2020;10(2):340.
- Zoehler B, Fracaro L, Senegaglia AC, Bicalho MDG. Infusion of mesenchymal stem cells to treat graft versus host disease: the role of HLA-G and the impact of its polymorphisms. *Stem cell Rev Rep*. 2020;16(3):459–71.
- Chen Y, Yu Q, Hu Y, Shi Y. Current research and use of mesenchymal stem cells in the therapy of autoimmune diseases. *Curr Stem Cell Res Ther*. 2019;14(7):579–82.
- Yousefi F, Lavi Arab F, Nikkhab K, Amiri H, Mahmoudi M. Novel approaches using mesenchymal stem cells for curing peripheral nerve injuries. *Life Sci*. 2019;221:99–108.
- Leng Z, Zhu R, Hou W, Feng Y, Yang Y, Han Q, Shan G, Meng F, Du D, Wang S, et al. Transplantation of ACE2(-) mesenchymal stem cells improves the outcome of patients with COVID-19 pneumonia. *Aging Dis*. 2020;11(2):216–28.
- Guo G, Zhuang X, Xu Q, Wu Z, Zhu Y, Zhou Y, Li Y, Lu Y, Zhang B, Talbot P, et al. Peripheral infusion of human umbilical cord mesenchymal stem cells rescues acute liver failure lethality in monkeys. *Stem Cell Res Ther*. 2019;10(1):84.
- Whitehead J, Zhang J, Harvestine JN, Kothambawala A, Liu GY, Leach JK. Tunneling nanotubes mediate the expression of senescence markers in mesenchymal stem/stromal cell spheroids. *Stem cells* (Dayton, Ohio). 2020;38(1):80–9.
- Banfi A, Muraglia A, Dozin B, Mastrogiacomo M, Cancedda R, Quarto R. Proliferation kinetics and differentiation potential of ex vivo expanded human bone marrow stromal cells: Implications for their use in cell therapy. *Exp Hematol*. 2000;28(6):707–15.
- Melzer C, Ohe JV, Hass R. Anti-tumor effects of exosomes derived from drug-incubated permanently growing human MSC. *Int J Mol Sci*. 2020;21(19):7311.
- Zhou X, Hong Y, Zhang H, Li X. Mesenchymal stem cell senescence and rejuvenation: current status and challenges. *Front Cell Dev Biol*. 2020;8:364.
- Sun X, Wang Z, Cong X, Lv Y, Li Z, Rong L, Yang T, Yu D. Mitochondrial gene COX2 methylation and downregulation is a biomarker of aging in heart mesenchymal stem cells. *Int J Mol Med*. 2021;47(1):161–70.
- Bertolo A, Baur M, Guerrero J, Pötzel T, Stoyanov J. Autofluorescence is a reliable in vitro marker of cellular senescence in human mesenchymal stromal cells. *Sci Rep*. 2019;9(1):2074.
- Lee HC, Kang D, Han N, Lee Y, Hwang HJ, Lee SB, You JS, Min BS, Park HJ, Ko YG, et al. A novel long noncoding RNA Linc-ASEN represses cellular senescence through multileveled reduction of p21 expression. *Cell Death Differ*. 2020;27(6):1844–61.
- Abdelmohsen K, Gorospe M. Noncoding RNA control of cellular senescence. *Wiley Interdiscip Rev RNA*. 2015;6(6):615–29.
- Guttman M, Rinn JL. Modular regulatory principles of large non-coding RNAs. *Nature*. 2012;482(7385):339–46.
- Montes M, Lund AH. Emerging roles of lncRNAs in senescence. *FEBS J*. 2016;283(13):2414–26.
- Kim J, Kim KM, Noh JH, Yoon JH, Abdelmohsen K, Gorospe M. Long noncoding RNAs in diseases of aging. *Biochem Biophys Acta*. 2016;1859(1):209–21.
- Li L, van Breugel PC, Loayza-Puch F, Ugalde AP, Korkmaz G, Messiga-Gold N, Han R, Lopes R, Barbera EP, Teunissen H, et al. LncRNA-OIS1 regulates DPP4 activation to modulate senescence induced by RAS. *Nucleic Acids Res*. 2018;46(8):4213–27.
- Dong J, Liu J, Wen Y, Tobin SW, Zhang C, Zheng H, Huang Z, Feng Y, Zhang D, Liu S, et al. Down-regulation of Lnc-CYP7A1-1 rejuvenates aged human mesenchymal stem cells to improve their efficacy for heart repair through SYNE1. *Front Cell Dev Biol*. 2020;8:600304.
- Cao Y, Sun Z, Liao L, Meng Y, Han Q, Zhao RC. Human adipose tissue-derived stem cells differentiate into endothelial cells in vitro and improve postnatal neovascularization in vivo. *Biochem Biophys Res Commun*. 2005;332(2):370–9.
- Fan L, Fan J, Liu Y, Li T, Xu H, Yang Y, Deng L, Li H, Zhao RC. miR-450b promotes osteogenic differentiation in vitro and enhances bone formation in vivo by targeting BMP3. *Stem Cells Dev*. 2018;27(9):600–11.
- Fan J, An X, Yang Y, Xu H, Fan L, Deng L, Li T, Weng X, Zhang J, Chunhua Zhao R. MiR-1292 targets FZD4 to regulate senescence and osteogenic differentiation of stem cells in TE/SJ/mesenchymal tissue system via the Wnt/beta-catenin pathway. *Aging Dis*. 2018;9(6):1103–21.
- Yang Y, Fan J, Xu H, Fan L, Deng L, Li J, Li D, Li H, Zhang F, Zhao RC. Long noncoding RNA LYPLAL1-AS1 regulates adipogenic differentiation of human mesenchymal stem cells by targeting desmoplakin and inhibiting the Wnt/beta-catenin pathway. *Cell Death Discov*. 2021;7(1):105.
- Xiao T, Liu L, Li H, Sun Y, Luo H, Li T, Wang S, Dalton S, Zhao RC, Chen R. Long noncoding RNA ADINR regulates adipogenesis by transcriptionally activating C/EBPalpha. *Stem Cell Rep*. 2015;5(5):856–65.

31. Li H, Fan J, Fan L, Li T, Yang Y, Xu H, Deng L, Li J, Li T, Weng X, et al. miRNA-10b reciprocally stimulates osteogenesis and inhibits adipogenesis partly through the TGF- $\beta$ /SMAD2 signaling pathway. *Aging Dis.* 2018;9(6):1058–73.
32. Xu M, Su X, Xiao X, Yu H, Li X, Keating A, Wang S, Zhao RC. Hydrogen peroxide-induced senescence reduces the wound healing-promoting effects of mesenchymal stem cell-derived exosomes partially via miR-146a. *Aging Dis.* 2021;12(1):102–15.
33. Li J, Yang Y, Fan J, Xu H, Fan L, Li H, Zhao RC. Long noncoding RNA ANCR inhibits the differentiation of mesenchymal stem cells toward definitive endoderm by facilitating the association of PTBP1 with ID2. *Cell Death Dis.* 2019;10(7):492.
34. Chu C, Quinn J, Chang HY. Chromatin isolation by RNA purification (ChIRP). *J Vis Exp JoVE.* 2012;61:3912.
35. Hahn HJ, Kim KB, An IS, Ahn KJ, Han HJ. Protective effects of rosmarinic acid against hydrogen peroxide-induced cellular senescence and the inflammatory response in normal human dermal fibroblasts. *Mol Med Rep.* 2017;16(6):9763–9.
36. Schmeer C, Kretz A, Wengerodt D, Stojiljkovic M, Witte OW. Dissecting aging and senescence-current concepts and open lessons. *Cells.* 2019;8(11):1446.
37. Zhou TE, Zhu T, Rivera JC, Omri S, Tahiri H, Lahaie I, Rouget R, Wirth M, Nattel S, Lodygensky G, et al. The inability of the choroid to revascularize in oxygen-induced retinopathy results from increased p53/miR-Let-7b activity. *Am J Pathol.* 2019;189(11):2340–56.
38. Fan J, An X, Yang Y, Xu H, Fan L, Deng L, Li T, Weng X, Zhang J, Chunhua Zhao R. miR-1292 Targets FZD4 to regulate senescence and osteogenic differentiation of stem cells in TE/SJ/mesenchymal tissue system via the Wnt/ $\beta$ -catenin pathway. *Aging Dis.* 2018;9(6):1103–21.
39. Zhuang W, Ge X, Yang S, Huang M, Zhuang W, Chen P, Zhang X, Fu J, Qu J, Li B. Upregulation of lncRNA MEG3 promotes osteogenic differentiation of mesenchymal stem cells from multiple myeloma patients By targeting BMP4 transcription. *Stem cells (Dayton, Ohio).* 2015;33(6):1985–97.
40. Wang Q, Li Y, Zhang Y, Ma L, Lin L, Meng J, Jiang L, Wang L, Zhou P, Zhang Y. LncRNA MEG3 inhibited osteogenic differentiation of bone marrow mesenchymal stem cells from postmenopausal osteoporosis by targeting miR-133a-3p. *Biomed Pharmacother Biomed Pharmacother.* 2017;89:1178–86.
41. Yoon JH, Abdelmohsen K, Srikantan S, Yang X, Martindale JL, De S, Huarte M, Zhan M, Becker KG, Gorospe M. LincRNA-p21 suppresses target mRNA translation. *Mol Cell.* 2012;47(4):648–55.
42. Bao X, Wu H, Zhu X, Guo X, Hutchins AP, Luo Z, Song H, Chen Y, Lai K, Yin M, et al. The p53-induced lincRNA-p21 derails somatic cell reprogramming by sustaining H3K9me3 and CpG methylation at pluripotency gene promoters. *Cell Res.* 2015;25(1):80–92.
43. Kalwa M, Hänzelmann S, Otto S, Kuo CC, Franzen J, Jousen S, Fernandez-Rebollo E, Rath B, Koch C, Hofmann A, et al. The lncRNA HOTAIR impacts on mesenchymal stem cells via triple helix formation. *Nucleic Acids Res.* 2016;44(22):10631–43.
44. Yoon JH, Abdelmohsen K, Kim J, Yang X, Martindale JL, Tominaga-Yamanaka K, White EJ, Orjalo AV, Rinn JL, Kreft SG, et al. Scaffold function of long non-coding RNA HOTAIR in protein ubiquitination. *Nat Commun.* 2013;4:2939.
45. Qiu JJ, Wang Y, Ding JX, Jin HY, Yang G, Hua KQ. The long non-coding RNA HOTAIR promotes the proliferation of serous ovarian cancer cells through the regulation of cell cycle arrest and apoptosis. *Exp Cell Res.* 2015;333(2):238–48.
46. Huang J, Ke P, Guo L, Wang W, Tan H, Liang Y, Yao S. Lentivirus-mediated RNA interference targeting the long noncoding RNA HOTAIR inhibits proliferation and invasion of endometrial carcinoma cells in vitro and in vivo. *Int J Gynecol Cancer.* 2014;24(4):635–42.
47. Sui BD, Zheng CX, Li M, Jin Y, Hu CH. Epigenetic regulation of mesenchymal stem cell homeostasis. *Trends Cell Biol.* 2020;30(2):97–116.
48. Yang Y, Liu S, He C, Chen Z, Lyu T, Zeng L, Wang L, Zhang F, Chen H, Zhao RC. Long non-coding RNA regulation of mesenchymal stem cell homeostasis and differentiation: advances, challenges, and perspectives. *Front Cell Dev Biol.* 2021;9:711005.
49. Almalki SG, Agrawal DK. Key transcription factors in the differentiation of mesenchymal stem cells. *Differentiation.* 2016;92(1–2):41–51.
50. Sethe S, Scutt A, Stolzing A. Aging of mesenchymal stem cells. *Ageing Res Rev.* 2006;5(1):91–116.
51. Kim M, Kim C, Choi YS, Kim M, Park C, Suh Y. Age-related alterations in mesenchymal stem cells related to shift in differentiation from osteogenic to adipogenic potential: implication to age-associated bone diseases and defects. *Mech Ageing Dev.* 2012;133(5):215–25.
52. Lin H, Sohn J, Shen H, Langhans MT, Tuan RS. Bone marrow mesenchymal stem cells: aging and tissue engineering applications to enhance bone healing. *Biomaterials.* 2019;203:96–110.
53. Rosen CJ, Ackert-Bicknell C, Rodriguez JP, Pino AM. Marrow fat and the bone microenvironment: developmental, functional, and pathological implications. *Crit Rev Eukaryot Gene Expr.* 2009;19(2):109–24.
54. D'ippolito G, Schiller PC, Ricordi C, Roos BA, Howard GA. Age-related osteogenic potential of mesenchymal stromal stem cells from human vertebral bone marrow. *J Bone Miner Res.* 1999;14(7):1115–22.
55. Zhou S, Greenberger JS, Epperly MW, Goff JP, Adler C, Leboff MS, Glowacki J. Age-related intrinsic changes in human bone-marrow-derived mesenchymal stem cells and their differentiation to osteoblasts. *Aging Cell.* 2008;7(3):335–43.
56. Li Y, Wu Q, Wang Y, Li L, Bu H, Bao J. Senescence of mesenchymal stem cells (Review). *Int J Mol Med.* 2017;39(4):775–82.
57. Turinetti V, Vitale E, Giachino C. Senescence in human mesenchymal stem cells: functional changes and implications in stem cell-based therapy. *Int J Mol Sci.* 2016;17(7):1164.
58. Geissler S, Textor M, Kühnisch J, Könnig D, Klein O, Ode A, Pfitzner T, Adjaye J, Kasper G, Duda GN. Functional comparison of chronological and in vitro aging: differential role of the cytoskeleton and mitochondria in mesenchymal stromal cells. *PLoS ONE.* 2012;7(12):e52700.
59. Denu RA, Hematti P. Effects of oxidative stress on mesenchymal stem cell biology. *Oxid Med Cell Longev.* 2016;2016:2989076.
60. Nuttall ME, Gimble JM. Controlling the balance between osteoblastogenesis and adipogenesis and the consequent therapeutic implications. *Curr Opin Pharmacol.* 2004;4(3):290–4.
61. Veldhuis-Vlug AG, Rosen CJ. Mechanisms of marrow adiposity and its implications for skeletal health. *Metabolism.* 2017;67:106–14.
62. Tang T, Yang L, Cao Y, Wang M, Zhang S, Gong Z, Xiong F, He Y, Zhou Y, Liao Q, et al. LncRNA AATBC regulates Pinin to promote metastasis in nasopharyngeal carcinoma. *Mol Oncol.* 2020;14(9):2251–70.
63. Ren N, Jiang T, Wang C, Xie S, Xing Y, Piao D, Zhang T, Zhu Y. LncRNA ADAMTS9-AS2 inhibits gastric cancer (GC) development and sensitizes chemoresistant GC cells to cisplatin by regulating miR-223-3p/NLRP3 axis. *Aging.* 2020;12(11):11025–41.
64. Tao Y, Yue P, Miao Y, Gao S, Wang B, Leng SX, Meng X, Zhang H. The lncRNA MEG3/miR-16–5p/VGLL4 regulatory axis is involved in etoposide-induced senescence of tumor cells. *J Gene Med.* 2021;23(2):e3291.
65. Liu YW, Xia R, Lu K, Xie M, Yang F, Sun M, De W, Wang C, Ji G. LincRNA-NAFEZF1-AS1 represses p21 expression to promote gastric cancer proliferation through LSD1-Mediated H3K4me2 demethylation. *Mol Cancer.* 2017;16(1):39.
66. Lin C, Wang Y, Wang Y, Zhang S, Yu L, Guo C, Xu H. Transcriptional and posttranscriptional regulation of HOXA13 by lncRNA HOTTIP facilitates tumorigenesis and metastasis in esophageal squamous carcinoma cells. *Oncogene.* 2017;36(38):5392–406.
67. Rinn JL, Chang HY. Genome regulation by long noncoding RNAs. *Annu Rev Biochem.* 2012;81:145–66.
68. Mondal T, Subhash S, Vaid R, Enroth S, Uday S, Reinius B, Mitra S, Mohammed A, James AR, Hoberg E, et al. MEG3 long noncoding RNA regulates the TGF- $\beta$  pathway genes through formation of RNA-DNA triplex structures. *Nat Commun.* 2015;6:7743.
69. Zhang Y, Long Y, Kwok CK. Deep learning based DNA:RNA triplex forming potential prediction. *BMC Bioinformatics.* 2020;21(1):522.
70. Krol J, Loedige I, Filipowicz W. The widespread regulation of microRNA biogenesis, function and decay. *Nat Rev Genet.* 2010;11(9):597–610.
71. Ha M, Kim VN. Regulation of microRNA biogenesis. *Nat Rev Mol Cell Biol.* 2014;15(8):509–24.
72. Ng DW, Zhang C, Miller M, Palmer G, Whiteley M, Tholl D, Chen ZJ. cis- and trans-Regulation of miR163 and target genes confers natural variation of secondary metabolites in two Arabidopsis species and their allopolyploids. *Plant Cell.* 2011;23(5):1729–40.
73. Finnegan EF, Pasquinelli AE. MicroRNA biogenesis: regulating the regulators. *Crit Rev Biochem Mol Biol.* 2013;48(1):51–68.



74. He L, He X, Lim LP, de Stanchina E, Xuan Z, Liang Y, Xue W, Zender L, Magnus J, Ridzon D, et al. A microRNA component of the p53 tumour suppressor network. *Nature*. 2007;447(7148):1130–4.
75. Kim J, Inoue K, Ishii J, Vanti WB, Voronov SV, Murchison E, Hannon G, Abellovich A. A MicroRNA feedback circuit in midbrain dopamine neurons. *Science (New York, NY)*. 2007;317(5842):1220–4.
76. Ertekin S, Yildirim O, Dinç E, Ayaz L, Fidancı SB, Tamer L. Evaluation of circulating miRNAs in wet age-related macular degeneration. *Mol Vis*. 2014;20:1057–66.

### Publisher's Note

Springer Nature remains neutral with regard to jurisdictional claims in published maps and institutional affiliations.

**Ready to submit your research? Choose BMC and benefit from:**

- fast, convenient online submission
- thorough peer review by experienced researchers in your field
- rapid publication on acceptance
- support for research data, including large and complex data types
- gold Open Access which fosters wider collaboration and increased citations
- maximum visibility for your research: over 100M website views per year

**At BMC, research is always in progress.**

Learn more [biomedcentral.com/submissions](https://biomedcentral.com/submissions)

